SciMedCentral

Chemical Engineering & Process Techniques

Review Article

Nanoparticulate Pd-Sn Compounds Supported on Metal Oxides: Synthesis, Material and Catalytic Properties

Alex O. Ibhadon[1]* and Shaun K. Johnston[2]

[1]*Department of Chemical Engineering, University of Hull, UK*
[2]*Department of Chemistry, University of Hull, UK*

***Corresponding author**

Alex Ibhadon, Department of Chemical Engineering, University of Hull, UK, Email: a.o.ibhadon@hull.ac.uk

Submitted: 29 May 2017

Accepted: 30 August 2017

Published: 01 September 2017

ISSN: 2333-6633

Keywords

- Catalysis; Palladium; Hydrogenation; X-Ray diffraction; Spectroscopy

Abstract

The manufacture of chemicals requires innovation at the catalyst frontier so that processes can be developed with higher energy efficiency and increased facility of separation and recovery of products. Catalysts with high selectivity and activity control the overall efficiency of a process by avoiding unwanted side-reactions and increasing the conversion per unit time. Although processes catalysed by homogeneous catalysts have the advantage of offering better control and understanding of the reaction mechanism, their frequent dependence on expensive metals which are difficult to recover, often precludes their employment in large-scale applications. Heterogeneously catalysed reactions on the other hand, are not associated with problems regarding recycling and reuse of catalyst, contamination of products or intermediates. This work reports the synthesis, characterization and testing of Pd-Sn nanoalloy catalyst in the selective hydrogenation of 2-methyl-3-butyn-2-ol. Our results show that the Pd-Sn nanoalloy, of composition Pd2.8Sn, supported on ZnO (Pd2.8Sn/ZnO), offers very high activity and selectivity in the semi- hydrogenation of 2-methyl-3-butyn-2-ol to 2-methyl-3-buten-2-ol in the liquid phase. Under identical reaction conditions, Pd2.8Sn/ZnO shows activity, both turn-over frequency and activity normalized by Pd content, significantly higher than Pd/CaCO3 (the Lindlar catalyst), with *TOF* of 137.6 s−1 compared to 79.2 s−1 for Pd/CaCO3 with approximately equal selectivity. The preparation of Pd2.8Sn/ZnO is achieved using a one-pot polyol procedure with the addition of a capping agent (polyvinylpyrrolidone) to control the particle size distribution. TEM shows nanoparticles evenly dispersed on the support, with a size distribution of 4.06 ± 0.75 nm. Single phase Pd2.8Sn was also prepared without the ZnO support, *via* the polyol method. Powder X-Ray diffraction data from the unsupported nanoalloy shows that the unit cell of Pd2.8Sn is face centred cubic with the Pd and Sn atoms occupying randomly the same crystallographic position. The chemical formula was calculated from a combination of ICP and PXRD analyses.

INTRODUCTION

Catalysts with high selectivity and activity are required in a vast array of synthetic processes and reactions. In particular, the synthesis of fine chemicals such as fragrances, pharmaceuticals, vitamins and complex agrochemicals, still relies on catalysts developed over six decades ago. The increased environmental awareness regarding synthetic reactions and chemical processing means that these materials now require significant improvement in both environmental footprint and performance. An example of these catalytic reactions is selective hydrogenation reaction-the hydrogenation of a carbon-carbon triple bond to a double bond, avoiding over-hydrogenation to a single bond. Selective hydrogenation is one of the critical reaction steps in the synthesis of vitamins A and E, the fragrance compound linalool and other important compounds [1]. The selective hydrogenation of 2-methyl-3-butyn-2-ol (MBY) to 2-methyl-3-buten-2-ol (MBE) as in Figure 1 (a), whilst avoiding successive [reaction (a) followed by reaction (b)], or direct full hydrogenation to 2-methylbutan-2-ol (MBA) (c), is an important starting reaction in industry [2] and is widely used as a model substrate to screen for activity and selectivity of catalyst materials in selective hydrogenation reactions [3].

Palladium-based catalysts in semi-hydrogenation reactions are active and more selective than other platinum-group metals [4], but their selectivity towards alkene products is still limited due to over-hydrogenation to alkanes and other side reactions such as dimerization and oligomerization reactions [5,6]. The widely used Pd/CaCO3 catalyst [6] (Pb poisoned with Pd supported on CaCO3), shows lower over-hydrogenation rate, while the addition of quinoline has been found to almost completely stop the formation of alkanes [7]. The exact mechanism by which the Pd/CaCO3 catalyst achieves its high selectivity is still unclear, however some literature have attributed it to a combination of electronic (or ligand) effects and active site isolation by the adsorption of poisons to the surface [8]. The presence of Pb adatoms and quinoline imparts electronic effects that minimize the formation of the Pd-H phase and effectively reduces the amount of adsorbed hydrogen as well as relative adsorption constants of alkyne and alkene molecules [9]. Moreover, the presence of Pb and quinoline minimizes the presence of Pd ensembles (active site isolation) that facilitate side-reactions [8]. The Pd/CaCO3 catalyst has been used for many years and, to date, still continues to be the most widely used selective hydrogenation catalyst on an industrial scale [10]. However, there are drawbacks associated with the use of Pd/

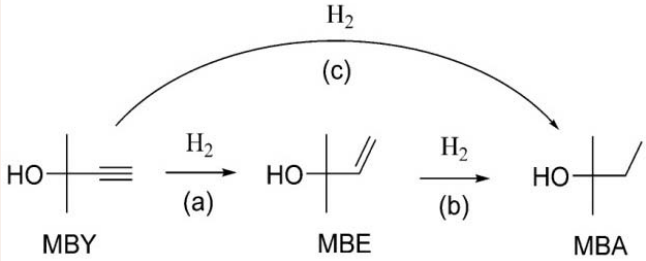

Figure 1 Reaction scheme of the hydrogenation of MBY to MBA. (MBY = 2-methyl-3-butyn-2-ol, MBE = 2-methyl-3-butene-2-ol and MBA = 2-methylbutan-2-ol.).

CaCO3 catalyst, the most prominent being the presence of lead, which causes increasing environmental concern, and the need for quinoline as an additional poison which hence leads to additional separation steps, consuming time and energy in the process [11]. Furthermore, the performance of the Lindlar catalyst in alkyne hydrogenations, although good, leaves plenty of room for improvement to allow for faster turnover of the desired product per catalyst amount such that less reaction time is needed.

In the search for more environmentally-friendly catalysts, many Pd-based alloy materials have been tested in the literature as alternative selective hydrogenation catalysts, utilising alternative co-metals such as Ag [12], Cu [13], Fe [14], Zn [15], Zr [16], and Ni [17]. The use of alloys can offer a significant selectivity improvement compared to Pd alone, due to electronic effects brought in by the presence of an additional atom and to active site isolation due to dilution of the Pd [18]. Palladium-tin compounds, in particular, have been used as catalysts for electro-oxidation reactions [19] and water de-nitration [20]. Catalysts composed of Pd and Sn in contact with each other and deposited on SiO2 supports, have been used in the selective hydrogenations of cinnamaldehyde [21], and PdxSny materials have been tested in selective hydrogenation of crotonaldehyde [22], with high selectivity in the former case being attributed to the suppression of C=C bond adsorption on the surface of the catalyst. In the selective hydrogenation of hexa- and butadienes, Pd-Sn compounds demonstrate remarkable selectivities, which have been attributed to the destruction of Pd ensembles by Pd-Sn bond formation [23], in addition to electronic effects, as the alloying of Pd with Sn has been shown to alter the electronic structure of the material [24]. A mixture of Pd-Sn compounds have also been reported recently to show promise in the catalysis of the gas phase semihydrogenation of acetylene [25].

Due to the 'promotion properties' imparted by Sn as a co-metal alongside Pd, and the promising results reported for a range of other hydrogenation reactions, we decided to investigate and test the Pd-Sn system which includes: PdSn4, PdSn3, PdSn2, α and β Pd3Sn2, PdSn, Pd2Sn and Pd3Sn. We focused our studies on Pd3Sn, the composition of which was reported to range between Pd3.26Sn and Pd2.85Sn, showing a cubic face centred unit cell throughout [26]. We prepared nanoparticles of a Pd3Sn-type random alloy with composition Pd2.8Sn, hence around the lower limit of the solid solution reported. We prepared the nanoparticles on ZnO support and tested this catalyst in the liquid phase semihydrogenation of MBY.

Experimental section

The preparation of Pd2.8Sn supported on ZnO was carried out using a one-pot polyol method involving the co-reduction of each precursor in the presence of support and by annealing to induce alloy formation. All materials were used as purchased. For the preparation of the Pd2.8Sn/ZnO catalyst, the metal precursors, palladium acetylacetonoate and tin acetylacetonoate each in 100 mL ethylene glycol and of molar concentration of 0.100 and 0.033M, respectively, were combined into the reaction vessel and ZnO support (200 mesh powder) was added alongside 1.000 g of PVP (average mol. Wt. 40000 g mol-1). The amount of support used was calculated to achieve 2 wt. % Pd loading (assuming all Pd (II) reduces to metal and deposits onto the support). The mixture was stirred under nitrogen gas flow at room temperature for at least 30 minutes to displace air before heating to reflux (196°C) for 3 hours. The mixture was cooled and the resulting black solid was obtained from the reaction mixture by centrifugation, washed with acetone (3 x 30 mL) and dried in an oven at 80°C in air for 30 minutes to yield a grey powder. Unsupported Pd2.8Sn nanoparticles for structural characterisation were prepared using the same method with exclusion of the support.

Selective hydrogenation procedure

Freshly-prepared catalysts (50 mg) and a hexane solution (100 mL) containing 0.741 g of butan-1-ol used as an internal standard, were transferred into a 250 mL 3-neck round bottom flask fitted with a rubber septum, thermometer and reflux condenser. A Schlenk line was connected through the top of the condenser to enable alternation between hydrogen gas, nitrogen gas, and vacuum.

The contents of the flask were stirred at 1100 rpm and heated to 50°C (temperature was controlled using a water bath and a temperature controller, providing the stability better than ± 0.1°C). Air from the reactor and the solvent was removed by purging the reactor 3 times with nitrogen gas - the pressure was slowly decreased until the solvent started to boil, and the reactor was filled with nitrogen gas. Nitrogen gas was then similarly substituted by hydrogen gas, purging the reactor 3 times. The contents were left stirring under hydrogen atmosphere (ambient pressure) for approximately 30 minutes to ensure the solvent and catalyst were saturated with hydrogen, and that no leak was present in the system (the hydrogen consumption was measured by a 300 mL gas burette). The reaction was started by quickly injecting 1.00 g MBY using a syringe through the septum. Aliquots of approximately 150 μL were taken at regular intervals with the increased sampling rate when the reaction approached 100% conversion (estimated using hydrogen consumption). Analysis of the products was performed using a Varian 430 gas chromatograph equipped with a 30 m Stabilwax® capillary column (Restek). The conversion of MBY (XMBY) and selectivity to MBE (SMBE, x) at different levels of conversion were calculated using the Equations (1-2), where CMBY, CMBE, CMBA and Cx are the concentrations of MBY, MBE, MBA and the concentrations at x% MBY conversion, respectively. These formulae imply that no components other than MBY, MBE and MBA were obtained, which was confirmed as no other peaks were observed on the chromatograms and the carbon balance for all reactions was 100 ± 2%.

$$X_{MBY} = \frac{C_{MBE} + C_{MBA}}{C_{MBY} + C_{MBE} + C_{MBA}} \quad (1)$$

$$S_{MBE,x} = \frac{C^{X}_{MBE}}{C^{X}_{MBE} + C^{X}_{MBA}} \quad (2)$$

The activity of the catalysts was characterized per mol. of Pd (A) using the average MBY consumption rate in 0-80% MBY conversion interval as in Equation (3), where ^{80} is the MBY conversion close to 80% occurred during the reaction time of ^{80}, ^{80} is the initial MBY concentration, is the solution volume, is the catalyst mass taken with Pd content of, and is the molar mass of Pd.

$$A = \frac{1 - X^{80}_{MBY}}{t^{80}_{MBY}} \frac{C^{0}_{MBY} V_{sol} M_{Pd}}{m_{cat} \omega_{Pd}} \quad (3)$$

Turn-over frequency (*TOF*) was used to characterise the average activity of the catalyst normalized per active site. The *TOF* was calculated using Equation (4), where is the total molar CO uptake determined by CO chemisorption studies.

$$TOF = \frac{1 - X^{80}_{MBY}}{t^{80}_{MBY}} \frac{C^{0}_{MBY} V_{SOL}}{n_{COuptake}} \quad (4)$$

X-ray diffraction analysis

Powder X-ray diffraction (PXRD) was carried out using a PANalytical empyrean X-ray diffractometer using monochromatic Cu Kα1 radiation and line PIXcel detector, scanning in the 2θ range of 20-120°, step size 0.105° and step time 24000 seconds. Results were recorded using the instrument's built-in software. Rietveld refinement was performed using GSAS software with the EXPGUI interface [26].

Transmission Electron Microscopy measurements

Samples for transmission electron microscopy (TEM) were dispersed in ethanol using an ultrasonic bath and a drop of dispersion was deposited onto carbon-coated copper grids. Images were obtained using a Gatan Ultrascan 4000 digital camera with Digital Micrograph software, attached to a Jeol 2010 TEM instrument running at 200 kV. Nanoparticle size distributions were obtained studying 3-5 TEM microphotographs obtained from different areas of the catalyst sample, measuring the diameter of a total of 200-400 individual nanoparticles using Gatan Digital Micrograph software.

Scanning electron microscopy measurements

Scanning electron microscopy (SEM) study was performed on the Zeiss EVO 60 instrument Oxford Instruments Inca System 350 under the pressure of 10−2 Pa and an electron acceleration voltage of 20 kV. Catalyst powder was glued to the specimen holder and carbon-coated.

Surface areas and pore distributions were measured by using a TriStar 3000 Micrometrics surface area and porosity analyser using standard multipoint BET analysis and BJH pore distribution methods. All specimens were dried at 150°C for 3 hours in nitrogen flow before the measurements.

Carbon Monoxide Chemisorption measurements

The total uptake of CO was measured with a Micromeritics AutoChem 2910 apparatus. Prior to a measurement, the catalyst was reduced in hydrogen with the following programme: flushing with helium at room temperature for 10 minutes, reduction in hydrogen at 300°C (10°C/min) for 120 minutes, flushing with helium at 300°C for 30 min and then return to ambient temperature. The total CO uptake measurements were performed at 25°C by injecting pulses of CO utilizing 10 vol. % CO in Helium.

ICP Analysis

Palladium, tin and lead content of the catalysts was determined using a Perkin Elmer Optima 5300DV emission inductively coupled plasma (ICP) spectrometer. The samples were dissolved in the solution of HF/HCl/HNO3 in a 1/1/3 ratio, heated at 200°C for 10 minutes using microwave digestion system CEM MARS Xpress Plus, followed by the addition of the boric acid saturated aqueous solution to complex excess HF, and the vessels were heated again at 180 °C for 10 minutes. The solutions were diluted with water and analysed.

RESULTS AND DISCUSSION

Lead-poisoned Pd/CaCO3 catalyst has been an industrial standard for semihydrogenation reactions for more than 60 years, but the high toxicity of lead and its compounds raises environmental concerns. Hence, we focused on Pd-Sn compounds; as Sn belongs to the same chemical group as lead and shares some chemical similarities, while its toxicity is notably lower [27]. The preparation of intermetallic compounds and alloys is traditionally carried out via reaction of the metals at high temperature (T > 1000°C); however, Cable and Shaak have demonstrated the synthesis of similar platinum-tin intermetallic compound via the polyol method, which relies on far lower reaction temperatures [28]. The high boiling point of these solvents is usually sufficient for alloy formation in solvent. We adapted this method to the preparation of Pd2.8Sn supported on ZnO. Zinc Oxide was chosen as support because it has been reported to enhance selectivity in semihydrogenation reactions compared to other supports [3,29]. The synthetic method used in this work leads to the preparation of Pd2.8Sn nanoparticles supported on ZnO in a one-step single pot reaction, with the polyol solvent (often ethylene glycol [28,30] or glycerol [28]) acting as surfactant to prevent agglomeration and large particle size, and as reducing agent, when heated [28]. The capping agent PVP was added to the reaction mixture to control particle size and further reduce any agglomeration of the nanoparticles. As such, a thorough washing procedure, using acetone followed by water, was used to remove as much capping agent as possible from the prepared material without calcination, which can "burn off" the polymer, but can result in sintering of the nanoparticles as well as carbon deposits that can deactivate the catalyst [31].

TEM Analysis

The TEM micrograph, Figure 2, of Pd2.8Sn/ZnO, shows evenly dispersed nanoparticles on the support material, with no densely populated regions of agglomerates. This is presumably due to "anchoring" of the nanoparticles during synthesis, perhaps

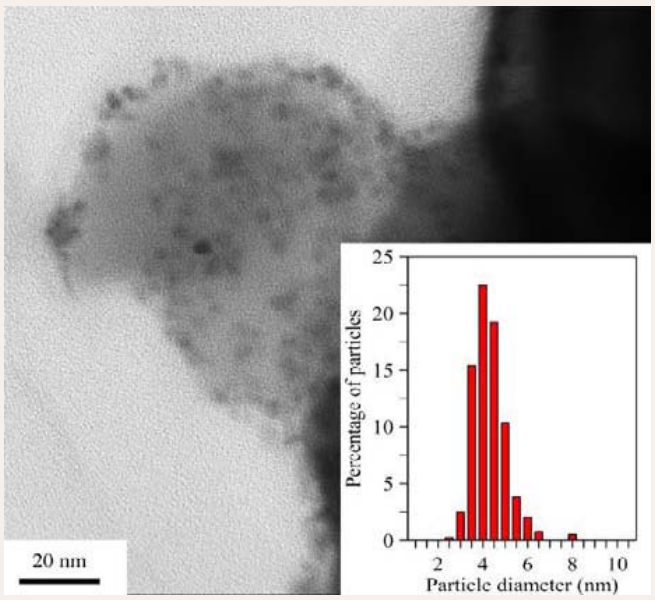

Figure 2 TEM micrograph of Pd2.8Sn/ZnO and particle size distribution histogram.

with nucleation preferentially occurring on the surface of ZnO and thus preventing agglomeration. The anchoring was likely caused by strong metal-support interactions between Pd-Sn and ZnO (Figure 2,3) [14,29,32].

The nanoparticles show a very narrow size distribution with average particle size = 4.06 nm (standard deviation = 0.75 nm). Commercial Pd/CaCO3 catalyst was also studied by TEM, but the analysis of catalyst particles supported on CaCO3 was difficult due to the large polycrystals of CaCO3 (an order of 10 μm), which prevented the electron beam from passing through the sample and consequently, SEM was used instead, Figure 3 In contrast to Pd2.8Sn/ZnO, Pd was very unevenly distributed on the Pd/CaCO3 catalyst support forming large micrometer-sized agglomerates in some areas, while very little metal was observed in other areas. Table 1 summarises the properties of the Pd2.8Sn/ZnO catalyst compared to Pd/CaCO3 catalyst. The catalysts have low specific surface area, because the support materials are crystalline and non-porous (Table 1).

Catalytic activity normalised per mol of Pd (*A*) and per active site (*TOF*) in the Pd2.8Sn/ZnO is about 2 times higher than in the Pd/CaCO3 catalyst despite the lower total Pd content. This effect can be explained as a combination of the following factors. Firstly, a promotion effect from Sn to Pd has been reported to suppress C=C adsorption on the catalyst surface compared to the bulk Pd present in the Pd/CaCO3 catalyst [20,24,33]. Secondly, there may be a further promotion effect from the ZnO support [3,29,34].

Figure 4 shows MBE selectivity as a function of MBY conversion for the studied catalysts. Pd2.8Sn/ZnO maintains between 97-98% selectivity even up to 99% conversion, and stays within approximately 0.5% of the selectivities shown by Pd/CaCO3 catalyst above 50% conversion under the same reaction conditions, likely due to the promotion with Sn and interaction with ZnO support, which led to the decrease in the alkene adsorption energy [20,24,33].

Both catalysts exhibit a sharp decrease in selectivity after approximately 95% conversion is reached, which can be attributed to an incomplete coverage of catalytic sites with MBY due to low concentration, freeing up sites for the less favoured MBE adsorption. This can be seen clearly in Figure 5, which shows the concentrations of MBY, MBE and MBA as a function of reaction time for Pd2.8Sn/ZnO and Pd/CaCO3 catalysts. In the Pd2.8Sn/ZnO catalysed reaction, there is very little MBA production until the vast majority of MBY has been converted to MBE, indicating no direct conversion of MBY to MBA (rather, over-hydrogenation to MBA occurs from hydrogenation of MBE in a separate step) in contrast to Pd/CaCO3 catalyst where there is some MBA production at lower MBY conversions.

To ensure the reaction is mediated by intrinsic kinetics (*i.e.* no extrinsic effects such as mass transfer limitations are affecting the reaction) the hydrogenation experiments were also carried out using twice as much catalyst (100 mg). This led to the reaction rate in all cases being doubled, with no difference in selectivity, as expected; hence only intrinsic kinetics has an effect on the reaction.

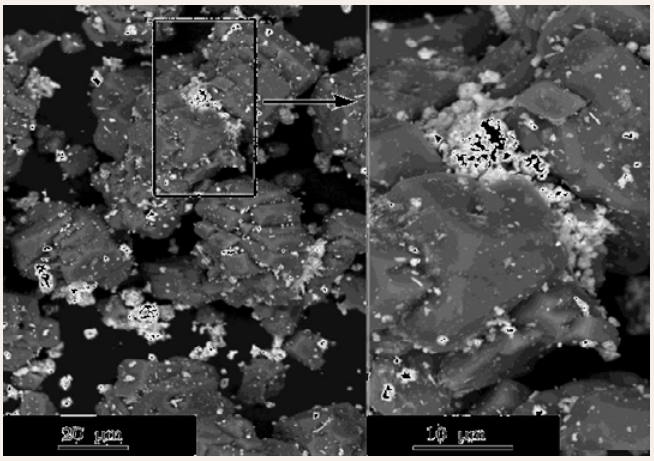

Figure 3 SEM micrographs of Pd/CaCO3 catalyst in electron backscattered mode at different magnifications.

Table 1: Comparison of the textural properties, elemental analysis and CO chemisorption data for the catalysts studied.

Catalyst	Pd/CaCO3	Pd2.8Sn/ZnO
SBET, m^2/g	1.8	9.3
Av pore	10.6	7.7
diameter		
(nm)[a]		
ICP Pd	4.22	2.15
Content (%)		
Molar metal	Pd/Pb=6.14	Pd/Sn=2.8
ratio		
A (s^{-1})	0.013	0.032
CO uptake,	14.6	6.6
μmol/g		
TOF (s^{-1})	79.2	137.6

To study the active component of the Pd2.8Sn/ZnO catalyst, unsupported Pd2.8Sn nanoparticles was carried out by PXRD and ICP analysis. ICP analysis gave a Pd:Sn ratio of 2.8:1. The PXRD pattern, Figure 6, confirmed that the compound prepared was a Pd3Sn-type nanoalloy by comparison with the patterns included in the Inorganic Cambridge Structural Database and also that secondary phases, such as SnO2, Sn metal or other Pd-Sn compounds, often found in previous work on Pd-Sn systems, were not present. Therefore we have obtained a single Pd-Sn compound with a Pd:Sn ratio of 2.8:1. This allowed us to conclude that the active component of our catalyst has the chemical formula Pd2.8Sn. The PXRD pattern was indexed using a face centred cubic unit cell, in agreement with previous reports on Pd3Sn, Figure 7 [35]. In this lattice, the Pd and Sn atoms are randomly distributed on the same crystallographic site (space group 3). The possibility of a primitive unit cell was also considered, as Malevskiy et al., reported a primitive unit cell, in analogy to the Pt-Sn system [36]. In a primitive lattice, (space group Pm3̄m), Pd and Sn atoms would occupy different crystallographic positions. The primitive unit cell corresponds to an intermetallic compound, while the face-centred unit cell corresponds to a random nanoalloy, according to a recent review by Sankar et al. [17], Systematic absences of reflections in X-Ray diffraction can be used to distinguish between primitive and face/body centred lattices.

For the face-centred cell, only the diffraction peaks with either all even or all odd Miller indices are observed, while the primitive cell shows all possible diffraction peaks. This means that the PXRD pattern of Pd2.8Sn with a primitive unit cell will show additional peaks when compared to the PXRD of Pd2.8Sn with a face centred unit cell. The PXRD patterns of Pd2.8Sn with a primitive and face centred unit cell were calculated and compared to the experimental PXRD pattern, Figure 6. The additional reflections in the PXRD pattern for the primitive unit cell are the (1 0 0) and (1 1 0) peaks in the 22 – 32 2θ degree region, the (2 1 0) and (2 1 1) peaks in the 51-57 2θ degree region and the (3 1 0) peak at ~ 57 2θ degrees. These diagnostic reflections are not present in the experimental PXRD pattern, leading to the conclusion that Pd2.8Sn, prepared via the polyol method, is a solid solution or a bimetallic random nanoalloy. The unit cell parameter and the Pd-Pd(Sn) distance were calculated via Rietveld refinement using the GSAS software with the EXPGUI interface [38] and found to be a = 3.949(3) Å, and Pd-Pd(Sn) = 2.7926(13) Å (Rwp = 0.098; Rp = 0.074 (see Supporting Information).

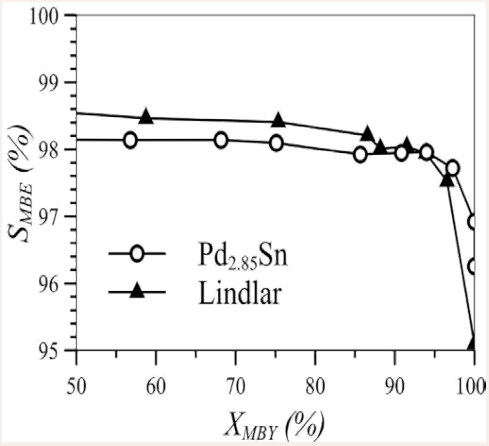

Figure 4 Conversion of MBY versus selectivity towards MBE on (O) Pd2.8Sn/ZnO and (▲) Lindlar catalyst at 50.0 ○C, 1 bar H2 pressure, 0.12M MBY solution in hexane.

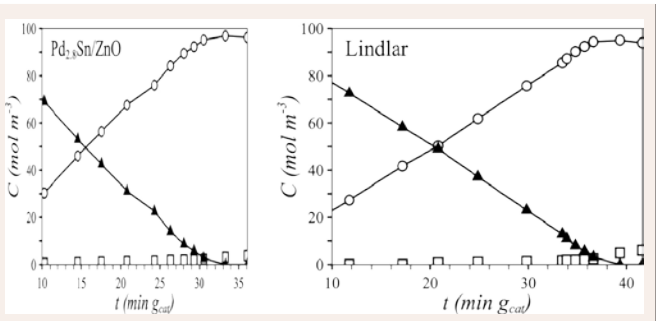

Figure 5 Concentrations of MBY (▲), MBE (O) and MBA (□) over time on (a) Pd2.8Sn/ZnO and (b) Pd/CaCO3 (Lindlar catalyst) at 50.0 ○C, 1 bar H2 pressure, 0.12M MBY solution in hexane.

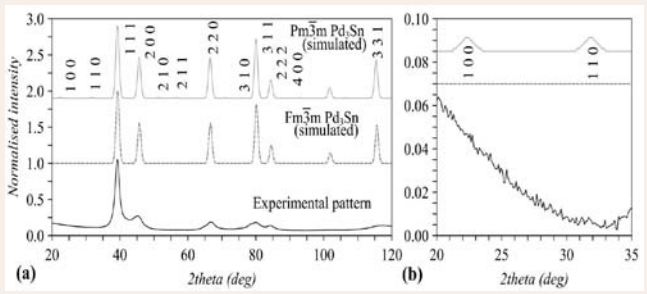

Figure 6 Comparison of the experimental PXRD pattern of unsupported Pd2.8Sn nanoparticles with simulated patterns of Pd2.8Sn having primitive cubic or face centred unit cells [34,35]. (a) Overall pattern and (b) one of the areas of diagnostic diffraction peaks magnified.

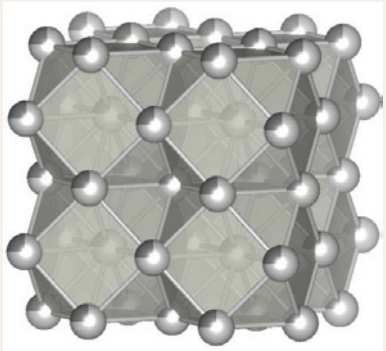

Figure 7 The structure of Pd2.8Sn, showing the random occupancy of Sn on the Pd crystal site. The colour light grey is associated to Pd atoms; the colour dark grey is associated to Sn atoms.

CONCLUSION

Pd2.8Sn nanoalloy supported on zinc oxide (Pd2.8Sn/ZnO) is proposed as a greener (lead-free) alternative to the Pd/CaCO3 catalyst, which is currently the most widely used catalyst for the semihydrogenation of acetylene alcohols at an industrial level, with significantly higher activity and comparable selectivity

(within 0.5 %). In the liquid phase semihydrogenation of MBY to MBE, the Pd2.8Sn/ZnO catalyst achieved 98% selectivity towards MBE even up to 95% MBY conversion without the use of any additional additives (poisons) in the reaction. We have also demonstrated significant improvement in the activity of the prepared catalyst, which shows a TOF of 137.6 s−1 compared to that of 79.2 s−1 exhibited by the Pd/CaCO3 catalyst (Pd/CaCO3). The synthesis was carried out using the polyol method. This route is based on low temperature (T < 200°C), compared to the more traditional preparation methods for alloys, which rely on temperatures above 1000°C and, furthermore, allowed the preparation of a single-phase Pd2.8Sn. TEM analysis showed the Pd2.8Sn/ZnO catalyst to consist of highly dispersed Pd2.8Sn nanoparticles on the ZnO support, with a very narrow size distribution (4.06 ± 0.75 nm). PXRD analyses of the unsupported materials prepared via the same method showed that Pd2.8Sn displays an all-face centred unit cell with Pd and Sn atoms randomly distributed on the same crystallographic position. Pd2.8Sn can, therefore, be considered a bimetallic random nanoalloy as opposed to an intermetallic compound.

ACKNOWLEDGEMENTS

We wish to acknowledge the use of the EPSRC funded National Chemical Database Service hosted by the Royal Society of Chemistry. We are grateful to Ann Lowry, Tony Sinclair and Bob Knight for TEM, SEM and ICP analyses, respectively.

REFERENCES

1. Ibhadon AO, Cherkasov N, McCue A, Anderson JA, Johnston SK. Palladium-bismuth intermetallic and surface-poisoned catalysts for the semi-hydrogenation of 2-methyl-3-butyn-2-ol. Appl Catal A Gen. 2015; 497: 22-30.
2. Cherkasov N, Ibhadon AO, Al-Rawashdeh M, Rebrov EV. Scale up study of capillary microreactors in solvent-free semihydrogenation of 2-methyl-3-butyn-2-ol. Catalysis Today. 2016; 273: 205-212.
3. Protasova LN, Rebrov EV, Choy KL, Pung SY, Engles V, Cabaj M, et al. ZnO based nanowires grown by chemical vapour deposition for selective hydrogenation of acetylene alcohols. Catal Sci Technol. 2011; 1: 768.
4. Rebrov EV, Klinger EA, Berenguer-Murcia A, Sulman EM, Schouten JC. Selective hydrogenation of 2-methyl-3-butyne-2-ol in a wall-coated capillary reactor with a Pd25Zn75/TiO_2 catalyst. Org Process Res Dev. 2009; 13: 991.
5. Ibhadon AO, Johnston SK. The Synthesis of Fine Chemicals Using Novel Catalysis. Synth Catal. 2017; 2: 4.
6. Nijhuis TA, Koten van G, Moulijn JA. Optimized palladium catalyst systems for the selective liquid-phase hydrogenation of functionalyzed alkynes. Appl Catal A Gen. 2003; 238: 259-271.
7. García-Mota M, Gómez-Díaz J, Novell-Leruth G, Vargas-Fuentes C, Bellarosa L, Bridier B, et al. A density functional theory study of the 'mythic' Lindlar hydrogenation catalyst. Theor Chem Acc. 2010; 128: 663-673.
8. Eggersdorfer M, Laudert D, Létinois U, McClymont T, Medlock J, Netscher T, et al. One hundred years of vitamins-a success story of the natural sciences. Angew Chem Int Ed Engl. 2012; 51: 12960-12990.
9. Anderson JA, Mellor J, Wells RPK. Pd catalysed hexyne hydrogenation modified by Bi and by Pb. J Catal. 2009; 261: 208.
10. Huang DC, Chang H, Pong WF, Tseng PK, Hung KJ, Huang WF. Effect of Ag-promotion on Pd catalysts by XANES. Catal Letters. 1998; 53: 155-159.
11. Boucher MB, Zugic B, Cladaras G, Kammert J, Marcinkowski MD, Lawton TJ, et al. Single atom alloy surface analogs in Pd0.18Cu15 nanoparticles for selective hydrogenation reactions. Phys Chem Chem Phys. 2013; 15: 12187-12196.
12. Guczi L, Schay Z, Stefler LF, Liotta LF, Deganello G, Venezia AM, et al. Pumice-Supported Cu–Pd Catalysts: Influence of Copper on the Activity and Selectivity of Palladium in the Hydrogenation of Phenylacetylene and But-1-ene. J Catal. 1999; 462: 456-462.
13. Wu JCS, Cheng T-S, Lai C-L. Boron nitride supported PtFe catalysts for selective hyderogenation of crotonaldehyde. Appl Catal A Gen. 2006; 314: 233-239.
14. Iwasa N, Takizawa M, Arai M. Preparation and application of nickel-containing smectite-type clay materials for methane reforming with carbon dioxide. Appl Catal A Gen. 2006; 314: 32-39.
15. Varga M, Molnár Á, Mohai M, Bertóti I, Janik-Czachor M, Szummer A. Selective hydrogenation of pentynes over PdZr and PdCuZr prepared from amorphous precursors. Appl Catal A Gen. 2002; 234: 167-178.
16. Sankar M, Dimitratos N, Miedziak PJ, Wells PP, Kiely CJ, Hutchings GJ. Designing bimetallic catalysts for a green and sustainable future. Chem Soc Rev. 2012; 41: 8099-8139.
17. Borodziński A, Nond GC. Selective Hydrogenation of Ethyne in Ethene-Rich Streams on Palladium Catalysts. Part 1. Effect of Changes to the Catalyst during Reaction. J Catal Rev. 2008; 50: 91-144.
18. He Q, Chen W, Mukerjee S, Chen S, Lufek F. Carbon-supported PdM (M = Au and Sn) nanocatalysts for the electrooxidation of ethanol in high pH media. J Power Sources. 2009; 187: 298-304.
19. Pintar A, Batista J, Muševič I. Palladium-copper and palladium-tin catalysts in the liquid phase nitrate hydrogenation in a batch-recycle reactor. Appl Catal B Environ. 2004; 52: 49-60.
20. Hammoudeh A, Mahmoud S. Selective hydrogenation of cinnamaldehyde over Pd/SiO_2 catalysts: selectivity promotion by alloyed Sn. J Mol Catal A Chem. 2003; 203: 231-239.
21. Protasova LN, Rebrov EV, Skelton HE, Wheatley AEH, Schouten JC. A kinetic study of the liquid-phase hydrogenation of citral on Au/TiO_2 and Pt–Sn/TiO_2 thin films in capillary microreactors. Appl Catal A Gen. 2011; 399: 12-21.
22. Cárdenas G, Oliva R, Reyes P, Rivas PL. Synthesis and properties of PdSn/Al_2O_3 and PdSn/SiO_2 prepared by solvated metal atom dispersed method. J Mol Catal A Chem. 2003; 191: 75-86.
23. Sales EA, Jove J, Mendes M de J, Bozon-Verduraz F. Palladium, Palladium–Tin, and Palladium–Silver Catalysts in the Selective Hydrogenation of Hexadienes: TPR, Mössbauer, and Infrared Studies of Adsorbed CO. J Catal. 2000; 195: 88-95.
24. Lee AF, Baddeley CJ, Tikhov MS, Lambert RM. Structural and electronic properties of Sn overlayers and PdSn surface alloys on Pd(111). Surf Sci. 1997; 373, 195-209.
25. Esmaeili E, Rashidi AM, Khodadadi AA, Mortazavi Y, Rashidzadeh M. Palladium–Tin nanocatalysts in high concentration acetylene hydrogenation: A novel deactivation mechanism. Fuel Process Technol. 2014; 120: 113-122.
26. Cable RE, Schaak RE. Reacting the unreactive: a toolbox of low-temperature solution-mediated reactions for the facile interconversion of nanocrystalline intermetallic compounds. J Am Chem Soc. 2006; 128: 9588-9589.
27. Tew MW, Emerich H, van Bokhoven JA. Formation and Characterization of PdZn Alloy: A Very Selective Catalyst for Alkyne Semihydrogenation.

J Phys Chem C. 2011; 115: 8457-8465.

28. Cable RE, Schaak RE. Low-Temperature Solution Synthesis of Nanocrystalline Binary Intermetallic Compounds Using the Polyol Process. Chem Mater. 2005; 17: 6835-6841.

29. Semagina N, Grasemann M, Xanthopoulos N, Renken A, Kiwi-Minsker L. Structured catalyst of Pd/ZnO on sintered metal fibers for 2-methyl-3-butyn-2-ol selective hydrogenation. J Catal. 2007; 251: 213-222.

30. Köhler D, Heise M, Baranov A, Luo Y, Geiger D, Ruck M, et al. Synthesis of BiRh Nanoplates with Superior Catalytic Performance in the Semihydrogenation of Acetylene. Chem Mater. 2012; 24: 1639-1644.

31. Wang G, Xiao L, Huang B, Ren Z, Tang X, Zhuang L, et al. AuCu intermetallic nanoparticles: surfactant-free synthesis and novel electrochemistry. J Mater Chem. 2012; 22: 15769.

32. Yarulin A, Yuranov I, Cárdenas-Lizana F, Alexander DTL, Kiwi-Minsker L. How to increase the selectivity of Pd-based catalyst in alkynol hydrogenation: Effect of second metal. Appl Catal A Gen. 2014; 478: 186-193.

33. Jung SM, Godard E, Jung SY, Park K, Choi JU. Liquid-phase hydrogenation of maleic anhydride over Pd–Sn/SiO_2. Catal Today. 2003; 87: 171-177.

34. Dominguez-Dominguez S, Berenguer-Murcia A, Linares-Solano A, Cazorla-Amoros D. Inorganic materials as supports for palladium nanoparticles: Application in the semi-hydrogenation of phenylacetylene. J Catal. 2008; 257: 87-95.

35. Breinlich C, Haubrich J, Becker C, Valcárcel A, Delbecq F, Wandelt K. Hydrogenation of 1,3-butadiene on Pd(111) and PdSn/Pd(111) surface alloys under UHV conditions. J Catal. 2007; 251: 123-130.

36. Zhang Q, Li J, Liu X, Zhu Q. Synergetic effect of Pd and Ag dispersed on Al_2O_3 in the selective hydrogenation of acetylene. Appl Catal A Gen. 2000; 197: 221-228.

37. Von Dreele RB, Larson AC. General structure analysis system (GSAS). 2004; 86-748

38. Toby BH. *EXPGUI*, a graphical user interface for *GSAS*. J Appl Crystallography. 2001; 34: 210-213.

Cite this article

Ibhadon AO, Johnston SK (2017) Nanoparticulate Pd-Sn Compounds Supported on Metal Oxides: Synthesis, Material and Catalytic Properties. Chem Eng Process Tech 3(3): 1044.